JACS
JOURNAL OF THE AMERICAN CHEMICAL SOCIETY
Communication
pubs.acs.org/JACS

Covalent Organic Frameworks Formed with Two Types of Covalent Bonds Based on Orthogonal Reactions

Yongfei Zeng,[†,§] Ruyi Zou,[†,§] Zhong Luo,[†] Huacheng Zhang,[†] Xin Yao,[†] Xing Ma,[†] Ruqiang Zou,*[,‡,§] and Yanli Zhao*[,†,§,∥]

[†]Division of Chemistry and Biological Chemistry, School of Physical and Mathematical Sciences, Nanyang Technological University, 21 Nanyang Link, Singapore 637371, Singapore

[‡]Department of Materials Science and Engineering, College of Engineering, Peking University, Beijing 100871, China

[§]Singapore Peking University Research Centre for a Sustainable Low-Carbon Future, 1 Create Way, Singapore 138602, Singapore

[∥]School of Materials Science and Engineering, Nanyang Technological University, Singapore 639798, Singapore

Supporting Information

ABSTRACT: Covalent organic frameworks (COFs) are excellent candidates for various applications. So far, successful methods for the constructions of COFs have been limited to a few condensation reactions based on only one type of covalent bond formation. Thus, the exploration of a new judicious synthetic strategy is a crucial and emergent task for the development of this promising class of porous materials. Here, we report a new orthogonal reaction strategy to construct COFs by reversible formations of two types of covalent bonds. The obtained COFs consisting of multiple components show high surface area and high H_2 adsorption capacity. The strategy is a general protocol applicable to construct not only binary COFs but also more complicated systems in which employing regular synthetic methods did not work.

As an emerging class of porous crystalline materials, covalent organic frameworks (COFs) whose structures can be precisely predetermined by molecular building blocks using reticular chemistry exhibit periodic architectures, low densities, and permanent porosity,[1] rendering them good candidates for various potential applications in gas adsorption,[2] optoelectronics,[3] catalysis,[4] separation,[5] and proton conduction.[6] Because the formation of strong covalent bonds usually affords poorly crystalline or amorphous compounds when connecting the molecular building blocks together, the construction of COFs with highly ordered structures and crystalline patterns needs the reversibility of condensation reactions during the synthesis. So far, all of the successful methods to construct COFs have only been limited to a few condensation reactions, including the formation of B−O (boronate, boroxine, and borosilicate),[7] C═N (imine, hydrazine, and squaraine),[8] C−N (triazine and imide),[9] B−N (borazine),[10] and N═N (azodioxide)[11] bond linkages. Furthermore, the COFs reported were built by only one type of covalent bond formation, with an exceptional example to boronate and boroxine due to competitive production of boronic acid.[12] Thus, the development of new judicious strategy and the exploration of synthetic methodology are crucial and emergent tasks for advancing the research progress of this new class of porous materials.

The concept of orthogonality was first applied in chemistry to protect amino acids in peptide synthesis[13] and then was extensively utilized in supramolecular chemistry through different interactions.[14] Among them, the orthogonal reactions usually involve reversible formations of covalent bonds, which are also an important prerequisite for the construction of crystalline porous COFs. Considering the documented COFs involving the formation of only one type of covalent bond at current stage, two types of organic reactions should be orthogonal (interference-free) in the dynamic process in order to construct predesigned COFs built from two covalent bonds. We hypothesized that this orthogonal reaction strategy, from which reversible formations of two types of covalent bonds were reported in supramolecular chemistry,[15] can be applicable to construct COFs with predetermined structures by rational choice of building blocks. It is worth pointing out that this strategy to prepare COFs is much more different from the reported Lewis acid-catalyzed protocol,[16] co-condensation method,[17] and competitive procedure.[12]

To apply orthogonal reaction strategy in COFs, one of the building blocks consisting of at least two functional groups is the premise for reversible formation of two types of covalent bonds (Scheme 1). One functional group can reversibly react with other building blocks, while the second one can dynamically self-condense (e.g., trimerize), to afford a two-component COF (Scheme 1a). However, the second group can also reversibly bond with the third building block to construct a three-component COF (Scheme 1b). Herein, the orthogonal reaction strategy was applied to construct not only binary COF (**NTU-COF-1**) but also ternary COF (**NTU-COF-2**), which involve the formations of two types of covalent bonds (Scheme 2). **NTU-COF-2**, the first multiple component COF reported so far, shows large Brunauer−Emmett−Teller (BET) surface area and high H_2 adsorption capacity.

The applicability of orthogonal reaction strategy was first actualized to construct a 2D COF (**NTU-COF-1**) by the formations of imine group and boroxine ring, involving the

Received: October 24, 2014
Published: January 12, 2015

DOI: 10.1021/ja510926w
J. Am. Chem. Soc. 2015, 137, 1020−1023

Scheme 1. Diagrams for the Constructions of (a) Binary and (b) Ternary COFs from Orthogonal Reaction Strategy; Both of Them Involve the Formation of Two Types of Covalent Bonds

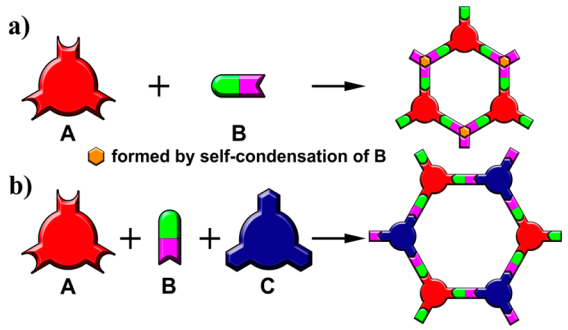

Scheme 2. Syntheses of (i) NTU-COF-1 and (ii) NTU-COF-2 Involving the Formation of Two Types of Covalent Bonds from Orthogonal Reactions; Attempts to Prepare NTU-COF-2 from (iii) NTU-COF-1, (iv) IM-1, and (v) IM-2, and Attempt to Prepare NTU-COF-1 from (vi) IM-1

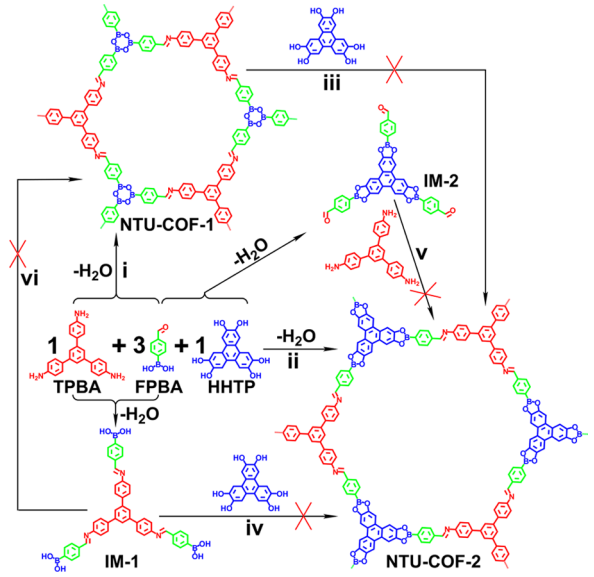

utilization of two building blocks of 4-formylphenylboronic acid (FPBA) and 1,3,5-tris(4-aminophenyl)-benzene (TAPB). FPBA contains ditopic groups of boronate and aldehyde. The former can be readily converted to boroxine ring under high temperature, while the latter can easily generate an imine group in the presence of amino group with nearly quantitative transformation. What is more crucial, these two reactions can be compatible in similar reaction conditions and do not interfere by each other, which make orthogonal reactions possible. **NTU-COF-1** was synthesized by solvothermal reaction of TAPB and FPBA in a 1:1 (v/v) mixture of 1,4-dioxane and mesitylene, followed by heating at 120 °C for 3 days, which afforded an orange crystalline solid in 85% yield (Scheme 2, route (i)). Fourier transform infrared (FT-IR) spectrum of **NTU-COF-1** (Figure S1) showed the disappearance of hydroxyl band stretching of boronic acid (3410 and 3212 cm^{-1}) in FPBA, indicating a completed conversion of boronic group, and the appearance of the B−O (1305 cm^{-1}), B−O (1336 cm^{-1}), B−C (1221 cm^{-1}), and B_3O_3 (711 cm^{-1}) bands corroborating the generation of B_3O_3 ring. Furthermore, the intensities for the C═O band (1668 cm^{-1}) and N−H band (3344−3462 cm^{-1}) in **NTU-COF-1** decreased significantly when compared with that of FPBA and TAPB, and a strong band of the imine group (C═N, 1627 cm^{-1}) emerged. Solid state ^{13}C cross-polarization magic-angle spinning (CP/MAS) NMR spectrum was conducted to confirm the precise connections in the structure of **NTU-COF-1** (Figure S3). The peak at ∼159 ppm is attributed to the imine carbon atom, formed by the condensation reaction of aldehyde group in FPBA and primary amine in TAPB. Field emission scanning electron microscopy (SEM) showed that **NTU-COF-1** crystallized in ball morphology (Figure S9).

To evaluate the adaptability of the strategy to complicated reaction systems, a novel three-component COF (**NTU-COF-2**) was designed and successfully constructed from three building blocks of FPBA, TAPB, and 2,3,6,7,10,11-hexadydroxytriphenylene (HHTP) through the formations of imine group and C_2O_2B boronate ring. **NTU-COF-2** was solvothermally synthesized by a mixture of TAPB, FPBA, and HHTP in 1,4-dioxane, followed by heating at 120 °C for 3 days, which gave a crystalline solid in 79% yield (Scheme 2, route (ii)). FT-IR spectrum of **NTU-COF-2** (Figure S2) showed that the hydroxyl band stretching of boronic acid (3410 and 3212 cm^{-1}) in FPBA is almost absent, indicating a completed consumption of boronic group. The appearance of the B−O (1403 cm^{-1}), B−O (1350 cm^{-1}), C−O (1253 cm^{-1}), and B−C (1017 cm^{-1}) bands supports the formation of C_2B_2O ring. Meanwhile, the carbonyl stretching band (1668 cm^{-1}) as well as the N−H stretching band (3344−3462 cm^{-1}) in **NTU-COF-2** strongly attenuated in comparison with those of FPBA and TAPB, and a new characteristic stretching band of the imine (C═N, 1623 cm^{-1}) group was observed. The atomic precision construction of **NTU-COF-2** was further verified by the solid state ^{13}C CP/MAS NMR (Figure S4). The peak at ∼157 ppm corresponds to the carbon atom of the imine bond, the formation of which is characteristic for the condensation reaction between aldehyde group in FPBA and primary amine in TAPB. SEM showed that **NTU-COF-2** crystallized with ball morphology, thus suggesting its phase purity (Figure S10).

To examine the stepwise method to prepare the two COFs, we attempted to use IM-1 to construct **NTU-COF-1**, as well as IM-1, IM-2 (Figures S5−S8), and **NTU-COF-1** to construct **NTU-COF-2** (Scheme 2, routes iii, iv, v and vi) in different solvent mixture ratios, respectively. However, no peaks were observed from powder X-ray diffraction (PXRD) patterns of the resulted products (Figures S16−S19), indicating the formation of amorphous solids, in spite that trace intermediates could be detected by HPLC (Figures S52−S54). Thus, the reaction mechanism for the formations of COFs was investigated through the exploration of the kinetics of COF growth. The *in situ* optical turbidity measurement, a fast but efficient technique developed by Dichtel et al. to explore COF-5 nucleation and growth process,[18] was utilized to study the growth kinetics of **NTU-COF-1** and **NTU-COF-2**. The formations of **NTU-COF-1** (27−33 kcal/mol) and **NTU-COF-2** (29−34 kcal/mol) need similar activation energies (Figures S32 and S34), while exhibiting second order and first order dependence on the concentrations with constant stoichiometric ratios of building blocks (FPBA/TAPB = 3/1 for **NTU-COF-1**; FPBA/TAPB/HHTP = 3/1/1 for **NTU-COF-2**), respectively (Figures S33 and S35), as compared to that of COF-5.[18] Notably, the formations of both COFs involve two types of covalent bonds. To make clear whether one bond was first generated or the two bonds were formed simultaneously, HPLC was executed to monitor the relative concentrations of building blocks (Figures S36−S39).

DOI: 10.1021/ja510926w
J. Am. Chem. Soc. 2015, 137, 1020−1023

The results demonstrate that the relative consumption rates of these building blocks are quite close to the stoichiometric ratios, revealing that the formations of **NTU-COF-1** and **NTU-COF-2** are a parallel mechanism, instead of a tandem process. Considering the generations of amorphous solids from IM-1 and IM-2, the parallel formations of imine and boronate/boroxine groups should be concurrently accompanied by the crystallization of COFs, followed by irreversible aggregations of crystallites that was observed in COF-5.[18] The proposed mechanism can well interpret the unsuccessful constructions of **NTU-COF-1** and **NTU-COF-2** from intermediate compounds via the step-by-step procedure.

The crystallinity of both **NTU-COF-1** and **NTU-COF-2** was also confirmed by PXRD analyses (Figures 1 and S12–S15).

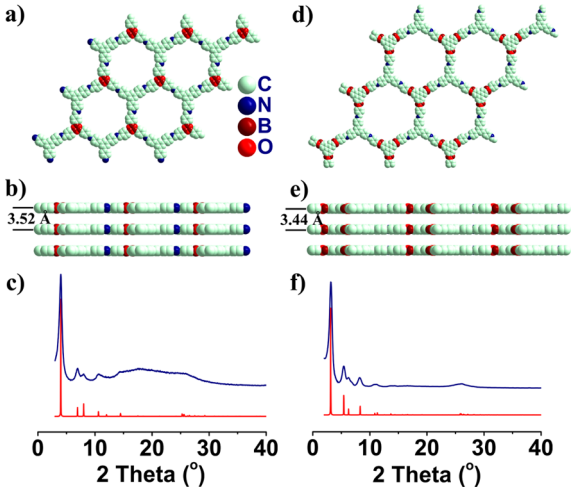

Figure 1. Simulated structures and PXRD patterns for **NTU-COF-1** (left) and **NTU-COF-2** (right). Views from (a,d) *c* axis and (b,e) *b* axis. The interlayer distances were determined by the simulation of a 2D eclipsed arrangement. H atoms were omitted for clarity. (c,f) Observed (navy) and simulated eclipsed stacking (red) PXRD patterns.

Their crystal structures were resolved by the PXRD profiles in conjunction with structural simulations (Figure 1). **NTU-COF-1** exhibits strong PXRD peaks at 4.02 (21.98 Å), 6.96 (12.70 Å), 8.04 (11.00 Å), 10.64 (8.31 Å), and 25.52° (3.49 Å), while **NTU-COF-2** at 3.08 (28.68 Å), 5.34 (16.55 Å), 6.16 (14.35 Å), 8.16 (10.83 Å), and 26.02° (3.43 Å), which can be assigned to the (100), (110), (200), (210), and (001) planes, respectively. The 2D extended structures in eclipsed stacking based on the space group $P\bar{6}$ (no. 174) were modeled for **NTU-COF-1** and **NTU-COF-2**. The unit cell parameters of $a = b = 25.469$ Å and $c = 3.526$ Å for **NTU-COF-1** and $a = b = 33.336$ Å and $c = 3.437$ Å for **NTU-COF-2** were calculated from geometrical energy minimization (Tables S1–S4). As expected, the simulated PXRD patterns from these two unit cells are in good agreement with the experimental PXRD patterns in terms of peak positions and relative intensities (Figures 1 and S22 and S26). Furthermore, the Pawley refinements based on their experimental PXRD patterns were carried out, which provided two good sets of factors of $wR_p = 4.37\%$ and $R_p = 3.42\%$ for **NTU-COF-1** and $wR_p = 4.47\%$ and $R_p = 3.14\%$ for **NTU-COF-2** (Figures S30 and S31). Except for eclipsed stacking, there were three different staggered PXRD patterns for the two COFs, which were also calculated (Figures S20 and S21). However, all of these calculated patterns did not match the experimental PXRD patterns (Figures S23–S25 and S27–29), excluding **NTU-COF-1** and **NTU-COF-2** from the staggered stacking modes.

Prior to porosity and gas uptake measurements, thermal gravimetric analysis was conducted to determine the thermal stability of **NTU-COF-1** and **NTU-COF-2** (Figure S11), showing that these two materials started to decompose at 300 and 350 °C, respectively. Thus, **NTU-COF-1** and **NTU-COF-2** were activated by degassing at 150 °C for 8 h, and then the intactness of the samples was verified by PXRD (Figures S40 and S41). Nitrogen gas (N_2) adsorption at 77 K was carried out to determine their permanent porosity. **NTU-COF-1** showed very low N_2 uptake and small surface area (Figures S42–S46), which may be due to the blockage of the pore channels by large fragments. **NTU-COF-2** exhibited a classic type IV isotherm characterized by a sharp uptake under low relative pressures at $P/P_0 < 0.01$ followed by a second step in $0.05 < P/P_0 < 0.20$, which is indicative of a mesoporous material (Figure 2a). The BET

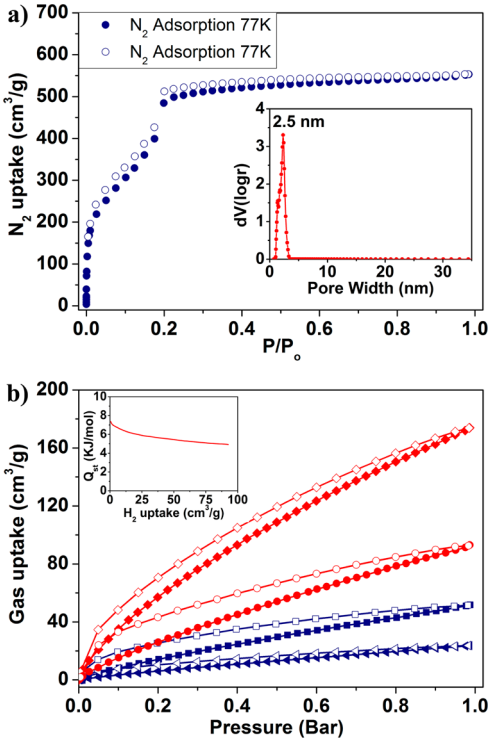

Figure 2. Gas adsorption isotherms of **NTU-COF-2**. (a) N_2 adsorption isotherm at 77 K. (Inset) pore size distribution by NLDFT. (b) H_2 adsorption isotherms at 77 (red ♦) and 87 K (red ●), and CO_2 adsorption isotherms at 273 (blue ■) and 298 K (blue ▲). (Inset) Isosteric heat of H_2 adsorption.

surface area of **NTU-COF-2** was evaluated by analysis of the low-pressure region ($0.05 \le P/P_0 \le 0.175$) of the isotherm, affording a value of 1619 $m^2\ g^{-1}$ (Figures S47–S49), which is larger than COF-5 (1590 $m^2\ g^{-1}$),[1a] TCOF-1 (927 $m^2\ g^{-1}$),[12] and DZnPc-ANDI-COF (1410 $m^2\ g^{-1}$),[19] and is comparable to COF-10 (1760 $m^2\ g^{-1}$),[2] ZnP-COF (1742 $m^2\ g^{-1}$),[20] and TT-COF (1810 $m^2\ g^{-1}$).[21] Its total pore volume was evaluated at $P/P_0 = 0.985$, which was $V_p = 0.86\ cm^3\ g^{-1}$. The pore-size distribution of **NTU-COF-2** was calculated on the basis of nonlocal density functional theory (NLDFT), revealing one type of 2.5 nm mesopore (Figure 2a, insert), which was in good agreement with the pore size predicted from the crystal structure (2.6 nm for **NTU-COF-2**).

DOI: 10.1021/ja510926w
J. Am. Chem. Soc. 2015, 137, 1020–1023

Because of the high surface area of **NTU-COF-2**, its hydrogen (H_2) and carbon dioxide (CO_2) adsorption was investigated to evaluate the potential application of this material in gas storage (Figure 2b). At 1.0 bar and 77 K, **NTU-COF-2** uptakes as high as 174 $cm^3\ g^{-1}$ (1.55 wt %) for H_2 (Figure 2b), which makes **NTU-COF-2** a top COF material for H_2 uptake reported to date, exceeding COF-1 (1.28 wt %), COF-5 (0.85 wt %),[1a] BLP-2(H) (1.5 wt %),[10] CTC−COF (1.12 wt %),[22] COF-102 (1.21 wt %), and COF-102 (1.29 wt %)[7a] and is comparable to CTF-1 (1.55 wt %)[9a] and TDCOF-5 (1.6 wt %).[23] The Q_{st} curve was calculated from the 77 and 87 K isotherms to provide a value of 7.3 kJ mol^{-1} at low coverage (Figure 2b, insert). This value is similar to those of 2D and 3D COFs, which usually lie between 5.0−8.0 kJ mol^{-1}.[24] CO_2 adsorption isotherms for **NTU-COF-2** were collected, showing that this material can store up to 10.2 wt % (51.8 $cm^3\ g^{-1}$) of CO_2 at 273 K and 1.0 bar, with Q_{st} value of 27.0 kJ mol^{-1} at low coverage (Figure S50).

In summary, we have developed a new strategy to construct novel COFs with the formations of two types of covalent bonds using orthogonal reactions. Not only can this strategy be adapted to binary systems but also to more complicated systems such as the first multiple-component **NTU-COF-2** that shows high BET surface area and large H_2 uptake capacity. The generality of this strategy was preliminarily conducted to afford a novel 2D COF (Figure S51). In particular, this orthogonal reaction strategy described exhibits the advantage over conventional step-by-step methods that cannot be validated to the two COFs. Given the limited condensation reactions and building blocks available to construct COFs, especially for COFs built from the single covalent bond at current stage, it can be expected that this protocol will broaden greatly the scope of the emerging materials.

■ ASSOCIATED CONTENT

Supporting Information

Synthetic procedures, FTIR, PXRD, solid state ^{13}C NMR, TGA, and SEM. This material is available free of charge via the Internet at http://pubs.acs.org.

■ AUTHOR INFORMATION

Corresponding Authors

*zhaoyanli@ntu.edu.sg

*rzou@pku.edu.cn

Notes

The authors declare no competing financial interest.

■ ACKNOWLEDGMENTS

This research is supported by the National Research Foundation (NRF), Prime Minister's Office, Singapore under its NRF Fellowship (NRF2009NRF-RF001-015) and CREATE Programme−Singapore Peking University Research Centre for a Sustainable Low-Carbon Future, and the NTU-A*Star Centre of Excellence for Silicon Technologies (A*Star SERC No.: 112 351 0003). R.Z. acknowledges National Natural Science Foundation of China (11175006 and 21371014) for financial support.

■ REFERENCES

(1) (a) Côté, A. P.; Benin, A. I.; Ockwig, N. W.; O'Keeffe, M.; Matzger, A. J.; Yaghi, O. M. *Science* **2005**, *310*, 1166. (b) Colson, J. W.; Dichtel, W. R. *Nat. Chem.* **2013**, *5*, 453. (c) Feng, X.; Ding, X.; Jiang, D. *Chem. Soc. Rev.* **2012**, *41*, 6010.

(2) Furukawa, H.; Yaghi, O. M. *J. Am. Chem. Soc.* **2009**, *131*, 8875.

(3) (a) Wan, S.; Guo, J.; Kim, J.; Ihee, H.; Jiang, D. *Angew. Chem., Int. Ed.* **2008**, *47*, 8826. (b) Dogru, M.; Bein, T. *Chem. Commun.* **2014**, *50*, 5531. (c) Liu, X. H.; Guan, C. Z.; Wang, D.; Wan, L. J. *Adv. Mater.* **2014**, *26*, 6912.

(4) (a) Ding, S.-Y.; Gao, J.; Wang, Q.; Zhang, Y.; Song, W.-G.; Su, C.-Y.; Wang, W. *J. Am. Chem. Soc.* **2011**, *133*, 19816. (b) Stegbauer, L.; Schwinghammer, K.; Lotsch, B. V. *Chem. Sci.* **2014**, *5*, 2789. (c) Fang, Q.; Gu, S.; Zheng, J.; Zhuang, Z.; Qiu, S.; Yan, Y. *Angew. Chem., Int. Ed.* **2014**, *53*, 2878.

(5) (a) Oh, H.; Kalidindi, S. B.; Um, Y.; Bureekaew, S.; Schmid, R.; Fischer, R. A.; Hirscher, M. *Angew. Chem., Int. Ed.* **2013**, *52*, 13219. (b) Ma, H.; Ren, H.; Meng, S.; Yan, Z.; Zhao, H.; Sun, F.; Zhu, G. *Chem. Commun.* **2013**, *49*, 9773.

(6) (a) Chandra, S.; Kundu, T.; Kandambeth, S.; BabaRao, R.; Marathe, Y.; Kunjir, S. M.; Banerjee, R. *J. Am. Chem. Soc.* **2014**, *136*, 6570. (b) Doonan, C. J.; Tranchemontagne, D. J.; Glover, T. G.; Hunt, J. R.; Yaghi, O. M. *Nat. Chem.* **2010**, *2*, 235.

(7) (a) El-Kaderi, H. M.; Hunt, J. R.; Mendoza-Cortes, J. L.; Côté, A. P.; Taylor, R. E.; O'Keeffe, M.; Yaghi, O. M. *Science* **2007**, *316*, 268. (b) Hunt, J. R.; Doonan, C. J.; LeVangie, J. D.; Côté, A. P.; Yaghi, O. M. *J. Am. Chem. Soc.* **2008**, *130*, 11872.

(8) (a) Uribe-Romo, F. J.; Hunt, J. R.; Furukawa, H.; Kloeck, C.; O'Keeffe, M.; Yaghi, O. M. *J. Am. Chem. Soc.* **2009**, *131*, 4570. (b) Uribe-Romo, F. J.; Doonan, C. J.; Furukawa, H.; Oisaki, K.; Yaghi, O. M. *J. Am. Chem. Soc.* **2011**, *133*, 11478. (c) Nagai, A.; Chen, X.; Feng, X.; Ding, X.; Guo, Z.; Jiang, D. *Angew. Chem., Int. Ed.* **2013**, *52*, 3770.

(9) (a) Kuhn, P.; Antonietti, M.; Thomas, A. *Angew. Chem., Int. Ed.* **2008**, *47*, 3450. (b) Fang, Q.; Zhuang, Z.; Gu, S.; Kaspar, R. B.; Zheng, J.; Wang, J.; Qiu, S.; Yan, Y. *Nat. Commun.* **2014**, *5*, 4503.

(10) Jackson, K. T.; Reich, T. E.; El-Kaderi, H. M. *Chem. Commun.* **2012**, *48*, 8823.

(11) Beaudoin, D.; Maris, T.; Wuest, J. D. *Nat. Chem.* **2013**, *5*, 830.

(12) Bertrand, G. H. V.; Michaelis, V. K.; Ong, T.-C.; Griffin, R. G.; Dinca, M. *Proc. Natl. Acad. Sci. U.S.A.* **2013**, *110*, 4923.

(13) Barany, G.; Merrifield, R. B. *J. Am. Chem. Soc.* **1977**, *99*, 7363.

(14) (a) Yan, X.; Cook, T. R.; Pollock, J. B.; Wei, P.; Zhang, Y.; Yu, Y.; Huang, F.; Stang, P. J. *J. Am. Chem. Soc.* **2014**, *136*, 4460. (b) Meyer, C. D.; Joiner, C. S.; Stoddart, J. F. *Chem. Soc. Rev.* **2007**, *36*, 1705. (c) Lehn, J.-M. *Chem. Soc. Rev.* **2007**, *36*, 151. (d) Ayme, J.-F.; Beves, J. E.; Leigh, D. A.; McBurney, R. T.; Rissanen, K.; Schultz, D. *Nat. Chem.* **2012**, *4*, 15. (e) Castilla, A. M.; Ramsay, W. J.; Nitschke, J. R. *Acc. Chem. Res.* **2014**, *47*, 2063. (f) Saha, M. L.; De, S.; Pramanik, S.; Schmittel, M. *Chem. Soc. Rev.* **2013**, *42*, 6860. (g) Hu, X.-Y.; Xiao, T.; Lin, C.; Huang, F.; Wang, L. *Acc. Chem. Res.* **2014**, *47*, 2041.

(15) (a) Icli, B.; Solari, E.; Kilbas, B.; Scopelliti, R.; Severin, K. *Chemistry* **2012**, *18*, 14867. (b) Christinat, N.; Scopelliti, R.; Severin, K. *Angew. Chem., Int. Ed.* **2008**, *47*, 1848. (c) Hutin, M.; Bernardinelli, G.; Nitschke, J. R. *Chemistry* **2008**, *14*, 4585.

(16) Spitler, E. L.; Dichtel, W. R. *Nat. Chem.* **2010**, *2*, 672.

(17) Bunck, D. N.; Dichtel, W. R. *Angew. Chem., Int. Ed.* **2012**, *51*, 1855.

(18) Smith, B. J.; Dichtel, W. R. *J. Am. Chem. Soc.* **2014**, *136*, 8783.

(19) Jin, S.; Ding, X.; Feng, X.; Supur, M.; Furukawa, K.; Takahashi, S.; Addicoat, M.; El-Khouly, M. E.; Nakamura, T.; Irle, S.; Fukuzumi, S.; Nagai, A.; Jiang, D. *Angew. Chem., Int. Ed.* **2013**, *52*, 2017.

(20) Feng, X.; Chen, L.; Dong, Y.; Jiang, D. *Chem. Commun.* **2011**, *47*, 1979.

(21) Dogru, M.; Handloser, M.; Auras, F.; Kunz, T.; Medina, D.; Hartschuh, A.; Knochel, P.; Bein, T. *Angew. Chem., Int. Ed.* **2013**, *52*, 2920.

(22) Yu, J.-T.; Chen, Z.; Sun, J.; Huang, Z.-T.; Zheng, Q.-Y. *J. Mater. Chem.* **2012**, *22*, 5369.

(23) Kahveci, Z.; Islamoglu, T.; Shar, G. A.; Ding, R.; El-Kaderi, H. M. *CrystEngComm* **2013**, *15*, 1524.

(24) Dawson, R.; Cooper, A. I.; Adams, D. J. *Prog. Polym. Sci.* **2012**, *37*, 530.

DOI: 10.1021/ja510926w
J. Am. Chem. Soc. 2015, 137, 1020−1023